Energy 51 (2013) 146–153

Contents lists available at SciVerse ScienceDirect

Energy

journal homepage: www.elsevier.com/locate/energy

An approximate expression for part-load performance of a microturbine combined heat and power system heat recovery unit

W. Rachtan, L. Malinowski*

Faculty of Maritime Technology and Transport, West Pomeranian University of Technology, Szczecin, 71-065 Szczecin, Al. Piastów 41, Poland

ARTICLE INFO

Article history:
Received 19 July 2012
Received in revised form
18 December 2012
Accepted 27 December 2012
Available online 4 February 2013

Keywords:
CHP
Microturbine
Part-load operation
Heat recovery
Approximate expression

ABSTRACT

An approximate expression for the heat transfer rate of a heat recovery unit (HRU) fed by the exhaust gas exiting a microturbine operating at part-load is developed. The proposed expression can be used for various microturbine-HRU sets if the appropriate values of coefficients are used. The independent variables in this expression are limited to: the microturbine electrical power output, the circulating water mass flow rate, and the circulating water inlet temperature. By the method of non-linear regression the coefficients of the approximate expression are determined for two types of microturbines and five types of HRUs. The developed expression greatly facilitates the prediction of available thermal power. Thus it can be useful in mathematical modeling of cogeneration plants based on microturbines as well as at the design and operation of such systems.

1. Introduction

Micro combined heat and power plants, especially those operating stand-alone, are subject to variable demand for electricity and heat. The amount of heat which can be recovered from exhaust gas in the heat recovery unit (HRU) depends on: the flow rate and temperature of exhaust gas, the flow rate and temperature of circulating water, and the type and size of HRU. When a specific microturbine is analyzed together with a specific HRU, the determination of heat transfer rate of the HRU for a given electrical output can be greatly simplified. The reason is that for specific environmental parameters the parameters of flue gas exiting the turbine and entering the HRU vary with the load in a strictly defined, unambiguous manner. Therefore there exists a possibility to formulate a function for calculating the heat transfer rate of the HRU, $\dot{Q}$, in which the independent variables are limited to: the microturbine electrical power output, P_{el}, the circulating water mass flow rate, $\dot{m}_w$, and the circulating water temperature at the inlet to the HRU, T_{w1}.

In this work the following structure of approximate expression for the heat transfer rate of the HRU,

$$\dot{Q} = \dot{Q}(P_{el}, \dot{m}_w, T_{w1}) \tag{1}$$

was established. Such an expression allows an easy and fast calculation of the amount of heat that can be recovered at different microturbine loads. It is a very useful tool for predicting the amount of heat available from HRU for a given electric load characteristics. It facilitates the development of such a strategy for operation of the microturbine-HRU system that will allow coverage of the demand for electricity and/or heat at any time. It is also useful for the variant selection of a microturbine-HRU set for the forecasted time varying demand for electricity and heat.

Coefficients appearing in expression (1) were determined based on the heat transfer rate of the HRU, calculated by the ε-NTU method for selected ranges of the microturbine electrical output, the circulating water mass flow rate, and the circulating water inlet temperature to the HRU.

In the literature considerable interest has been devoted to the micro combined heat and power (CHP) plants based on microturbines [1–9] or small internal combustion engines [10–16], operated at part-load. In their works the authors have paid much attention to the problems of exhaust heat recovery. They conducted experimental research [1–3,6,7,12–16] and computational analyses [2,4–6,8–11,16]. The aim of the investigations was to evaluate CHP plants in terms of their performance and energy efficiency [1–16]. In some cases the economic [4,5,8,10,14] or environmental [8,10,14,16] aspects of CHP were emphasized. The experimental works have shown a large impact of the engine load [1,3,6,7,12–15], circulating water flow rate [13], and circulating water temperature [1,12] on the amount of heat recovered in the HRU. In Ref. [3] the

* Corresponding author. Tel.: +48 91 449 4827.
E-mail addresses: lmal@zut.edu.pl, leszmali@gmail.com (L. Malinowski).

0360-5442/$ – see front matter © 2013 Elsevier Ltd. All rights reserved.
http://dx.doi.org/10.1016/j.energy.2012.12.037

Nomenclature

A	total heat transfer surface area, m^2
A_e	external tubes surface area, m^2
A_f	fins surface area, m^2
A_i	internal tubes surface area, m^2
A_{min}	minimum free-flow area, m^2
A_{wall}	average tubes surface area, m^2
B	finned breadth, m
c_w	specific heat at constant pressure of water, J kg^{-1} K^{-1}
C_1, C_2	coefficients
C^*	heat capacity rate ratio
C_{min}	smaller heat capacity rate for the two fluid streams (exhaust gas), $W\cdot^{-1}$
C_{max}	larger heat capacity rate for the two fluid streams (water), W K^{-1}
D_c	fin collar outside diameter (outer diameter of the tube increased by twice the fin thickness), m
D_h	hydraulic diameter, m
D_i	tube inside diameter, m
f_w	Fanning friction factor for water
F_p	fin pitch, m
h_{exh}	convection heat transfer coefficient for exhaust gas, W m^{-2} K^{-1}
h_w	convection heat transfer coefficient for water, W m^{-2} K^{-1}
H	finned height, m
i	data set number
$j1$, $j2$	expressions in Wang's correlation
j_H	Colburn factor for heat transfer
$J1$–$J3$	expressions in Wang's correlation
k_f	thermal conductivity of fins, W m^{-1} K^{-1}
k_w	thermal conductivity of water, W m^{-1} K^{-1}
k_{wall}	thermal conductivity of tubes wall, W m^{-1} K^{-1}
L	finned length, m
m	fin effectiveness parameter, m^{-1}
$\dot{m}_{exh}$	exhaust gas mass flow rate, kg s^{-1}
$\dot{m}_w$	circulating water mass flow rate, kg s^{-1}
n	number of data sets of a given case
N	number of tube rows
NTU	number of heat transfer units
Nu_{exh}	Nusselt number for exhaust gas
Nu_w	Nusselt number for water
P_{el}	electrical power output, W
P_l	longitudinal tube pitch, m
P_t	transverse tube pitch, m
Pr_{exh}	Prandtl number for exhaust gas
Pr_w	Prandtl number for water
q	heat per unit mass, J/kg
$\dot{Q}$	heat transfer rate of a heat recovery unit, W
$\dot{Q}_i$	heat transfer rate of a heat recovery unit calculated with the effectiveness-NTU method for the i-th data set, W
$\dot{Q}_{max}$	maximum possible heat transfer rate of a cross- and counterflow heat exchanger, defined by Eq. (31), W
r	tube inside radius, m
R_{eq}	equivalent radius for circular fin, m
Re_{Dc}	Reynolds number for exhaust gas with the characteristic dimension of the flow defined as the fin collar diameter D_c
Re_{Di}	Reynolds number for water with the characteristic dimension of the flow defined as the tube inside diameter D_i
RMS	root mean square error of correlation function (32), W
s	fin spacing (fin pitch minus fin thickness), m
S	weighted sum of relative errors
T_{exh1}	exhaust gas temperature at the inlet to HRU (at the outlet of the microturbine unit), K
T_{w1}	circulating water temperature at the inlet to HRU, K
T_{w2}	circulating water temperature at the outlet from HRU, K
UA	product of the overall heat transfer coefficient and total heat transfer surface area, W K^{-1}
w	weighting factor
X_f	wavy-fin pattern length, m

Greek letters

δ_f	fin thickness, m
δ_{wall}	tube wall thickness, m
ε	effectiveness of heat exchanger
η_f	fin efficiency
η_s	extended surface efficiency
θ	corrugation angle, °
Φ	fin effectiveness parameter

Abbreviations and acronyms

CHP	combined heat and power
HRU	heat recovery unit
NO REC	non-recuperated microturbine Capstone 330
REC	recuperated microturbine Capstone C30

significant influence of electrical load on the HRU effectiveness is highlighted. In the works in which computational analyses were carried out, the performance of HRU was determined based on the assumption that at all operating conditions the HRU exhaust gas outlet temperature is constant [4,5,8] or that the relative outlet losses are constant [10], whereas in Refs. [9,11] a detailed mathematical model of recovery heat exchanger was used. Particularly noteworthy are Refs. [4,5,9,11] in which generalized part-load performance characteristics of CHP microturbines or CHP internal combustion engines are developed. In Refs. [4,5] the CHP heating capacity is calculated on the assumption that the temperature of the flue gas exiting the HRU is in all cases equal to 70 °C. In the case of Refs. [9,11] the heat from the exhaust gas is utilized in a heat recovery steam generator. The part-load performance of the heat recovery steam generator was calculated in this case from special approximate expressions. These expressions concerning steam generators, as to the structure, functions arguments, and potential applications, are similar to those developed for water heaters in the present work.

2. Analysis

2.1. Rigorous model

The analysis comprises two types of commercially produced microturbines with a nominal power of 30 kW. One of them is the Capstone C30 microturbine operating according to a recuperated cycle, and the other is the Capstone 330 based on a non-recuperated cycle. Both turbines are operated at part load by reducing the rotational speed. The analysis is based on two microturbine part-load characteristics: the dependence of exhaust gas mass flow rate and the dependence of exhaust gas temperature

on the microturbine electrical power output. These characteristics are given, respectively, by Eqs. (2) and (3) for the recuperated microturbine Capstone C30 (REC) and by Eqs. (4) and (5) for the non-recuperated microturbine Capstone 330 (NO REC). They are valid for the ISO ambient conditions (15 °C, 60% relative humidity, 101.325 kPa standard sea level pressure) and steady-state part-load operation. In the development of correlations (2)–(5) the values of exhaust gas mass flow rate and exhaust gas temperature taken from manufacturer's technical files were used [17,18].

For the REC case

$$\dot{m}_{\mathrm{exh}} = 0.09100 + 0.01100\cdot P_{\mathrm{el}} - 2.325\times 10^{-4}\cdot P_{\mathrm{el}}^2 + 3.699 \times 10^{-6}\cdot P_{\mathrm{el}}^3 \quad (2)$$

$$T_{\mathrm{exh1}} = 2.887\cdot P_{\mathrm{el}} + 463.1 \quad (3)$$

For the NO REC case

$$\dot{m}_{\mathrm{exh}} = 0.09768 + 0.01242\cdot P_{\mathrm{el}} - 2.964\times 10^{-4}\cdot P_{\mathrm{el}}^2 + 4.480 \times 10^{-5}\cdot P_{\mathrm{el}}^3 \quad (4)$$

$$T_{\mathrm{exh1}} = 738.1 + 15.44\cdot P_{\mathrm{el}} - 2.157\cdot P_{\mathrm{el}}^2 + 0.1873\cdot P_{\mathrm{el}}^3 - 0.01020\cdot P_{\mathrm{el}}^4 + 3.331\times 10^{-4}\cdot P_{\mathrm{el}}^5 - 5.933\times 10^{-6}\cdot P_{\mathrm{el}}^6 + 4.418\times 10^{-8}\cdot P_{\mathrm{el}}^7 \quad (5)$$

In the correlations given by Eqs. (2)–(5) P_{el} [kW] ranges from 2 kW to 30 kW, $\dot{m}_{\mathrm{exh}}$ is expressed in [kg/s], and T_{exh1} in [K]. The relative errors of approximations do not exceed 3% at any data point.

Analyzed cases of the microturbine-HRU sets are listed in Table 1. Table 2 shows the data on the examined HRUs. Schematic bundle structure is shown in Fig. 1. Using the part-load characteristics of microturbines given by Eqs. (2)–(5) and the geometrical characteristics of the heat exchangers, values of the convection heat transfer coefficient on the exhaust gas side surface of the HRU were calculated for different loads. For the case of wavy fins the following correlation proposed by Wang et al. [19] was used.

For $Re_{D_c} < 1000$

$$j_{\mathrm{H}} = 0.882\cdot Re_{D_c}^{J1}\cdot\left(\frac{D_c}{D_h}\right)^{J2}\cdot\left(\frac{s}{P_t}\right)^{J3}\cdot\left(\frac{s}{D_c}\right)^{-1.58}\cdot\tan(\theta)^{-0.2} \quad (6)$$

Table 2
Characteristics of investigated HRUs.

Type of exchanger		
A tube-fin exchanger with flat plain (HRU type-1) or wavy-herringbone (HRU type-2) fins		
Tube bundle		
Type of tube bundles: staggered tube arrangement, multipass water flow – number of passes equal to number of tube rows, one-pass flow of exhaust gas, unmixed–unmixed.		
Nominal operating parameters (for rated power of the Capstone C30 microturbine)		
Water side		
Flow rate		5.50 m^3/h
Velocity		0.93 m/s
Exhaust gas side		
Face velocity (inlet 275 °C, 0.31 kg/s – nominal for C30)		2.7 m/s
HRU data		
	HRU type-1 (cases 1–6)	**HRU type-2 (cases 7–10)**
Name of bundle	P40-16	P30-12
Fin type	Plain	Wavy-herringbone
Tubes and fins material	Stainless steel AiSi316	Copper
Number of tube rows, N	4, 8 or 12	4 or 6
Finned surface area, A	16.636, 33.252 or 49.867 m^2	14.631 or 21.933 m^2
Number of tubes in a row	10	14
Tube outer diameter	16.5 mm	12.2 mm
Tube wall thickness, δ_{wall}	1.00 mm	0.5 mm
Finned breadth, B	440 mm	440 mm
Finned height, H	400 mm	420 mm
Finned length, L	138.56, 277.12 or 415.68 mm	120 mm or 180 mm
Fin thickness, δ_f	0.15 mm	0.20 mm
mm Fin pitch, F_p	2.60 mm	2.85 mm
Number of fins	168	153
Longitudinal tube pitch, P_l	34.64 mm	30 mm
Transverse tube pitch, P_t	40 mm	30 mm
Ratio of the minimum flow area to frontal area for exhaust gas	55.4%	55.2%

where

$$J1 = 0.0045 - 0.491\cdot Re_{D_c}^{-0.0316-0.0171\cdot\ln(N\cdot\tan(\theta))}\cdot\left(\frac{P_l}{P_t}\right)^{-0.109\cdot\ln(N\cdot\tan(\theta))}\cdot\left(\frac{D_c}{D_h}\right)^{0.542+0.0471\cdot N}\cdot\left(\frac{s}{D_c}\right)^{0.984}\cdot\left(\frac{s}{P_t}\right)^{-0.349} \quad (7)$$

$$J2 = -2.72 + 6.84\cdot\tan(\theta) \quad (8)$$

Table 1
Investigated cases of microturbine-HRU sets.

Case number	Type of HRU[a]	Number of tube rows, N	Finned surface area, A m^2	Finned length, L mm	Type of microturbine	Correlations for convection heat transfer coefficients	ε-NTU relationship	Correlations for microturbine performance
1	1	4	6.636	138.56	REC	Eqs. (14), (16) and (18)	Eq. (27)	Eqs. (2) and (3)
2.	1	8	33.252	277.12	REC	Eqs. (14), (16) and (18)	Eq. (26)	Eqs. (2) and (3)
3.	1	12	49.867	415.68	REC	Eqs. (14), (16) and (18)	Eq. (26)	Eqs. (2) and (3)
4.	1	4	16.636	138.56	NO REC	Eqs. (14), (16) and (18)	Eq. (27)	Eqs. (4) and (5)
5.	1	8	33.252	277.12	NO REC	Eqs. (14), (16) and (18)	Eq. (26)	Eqs. (4) and (5)
6.	1	12	49.867	415.68	NO REC	Eqs. (14), (16) and (18)	Eq. (26)	Eqs. (4) and (5)
7.	2	4	14.631	120	REC	Eqs. (6)–(12), (16), (18)	Eq. (27)	Eqs. (2) and (3)
8.	2	6	21.933	180	REC	Eqs. (6)–(12), (16), (18)	Eq. (27)	Eqs. (2) and (3)
9.	2	4	14.631	120	NO REC	Eqs. (6)–(12), (16), (18)	Eq. (27)	Eqs. (4) and (5)
10.	2	6	21.933	180	NO REC	Eqs. (6)–(12), (16), (18)	Eq. (27)	Eqs. (4) and (5)

[a] Types of HRUs are specified in Table 2.

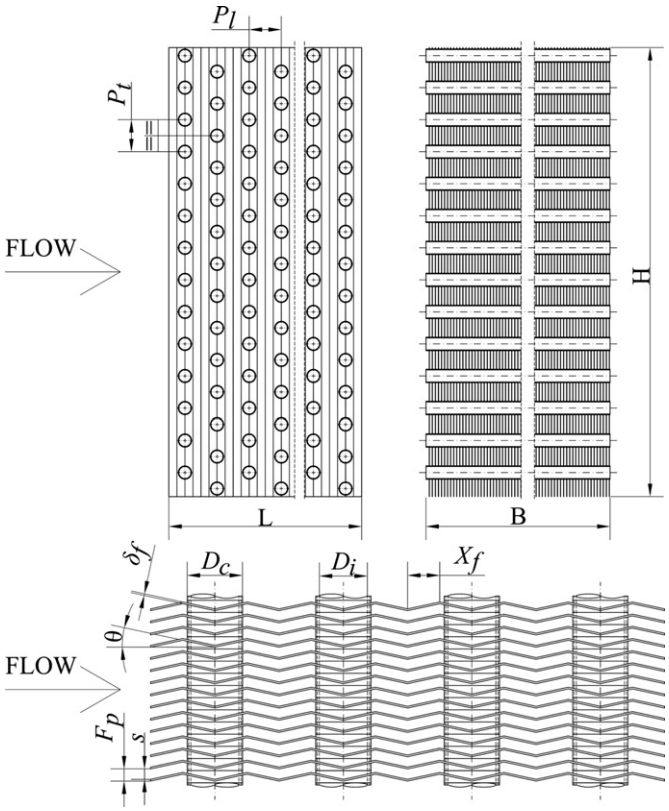

Fig. 1. Schematic wavy-fin bundle structure. For plain fins the corrugation angle, θ, is equal to zero.

$$J3 = 2.66\cdot\tan(\theta) \tag{9}$$

For $Re_{Dc} \geq 1000$

$$j_H = 0.0646\cdot Re_{Dc}^{j1}\cdot\left(\frac{D_c}{D_h}\right)^{j2}\cdot\left(\frac{s}{P_t}\right)^{-1.03}\cdot\left(\frac{P_l}{D_c}\right)^{0.432}\cdot\tan(\theta)^{-0.692}\cdot N^{-0.737} \tag{10}$$

where

$$j1 = -0.0545 - 0.0538\cdot\tan(\theta) - 0.302\cdot N^{-0.24}\cdot\left(\frac{s}{P_l}\right)^{-1.3}\cdot\left(\frac{P_l}{P_t}\right)^{0.379}\cdot\left(\frac{P_l}{D_h}\right)^{-1.35}\cdot\tan(\theta)^{-0.256} \tag{11}$$

$$j2 = -1.29\cdot\left(\frac{P_l}{P_t}\right)^{1.77-9.43\cdot\tan(\theta)}\cdot\left(\frac{D_c}{D_h}\right)^{0.229-1.43\cdot\tan(\theta)}\cdot N^{-0.166-1.08\cdot\tan(\theta)}\cdot\left(\frac{s}{P_t}\right)^{-0.174\cdot\ln(0.5\cdot N)} \tag{12}$$

Hydraulic diameter D_h is defined as

$$D_h = 4\cdot A_{min}\cdot L/A \tag{13}$$

These expressions are valid for

$Re_{Dc} = 300 - 10,000$

$D_c = 7.66 - 16.85$ mm

$P_t = 21 - 38.1$ mm

$P_l = 12.7 - 33$ mm

$F_p = 1.21 - 6.43$ mm

$N = 1 - 6$

$\theta = 5.3 - 18.5°$

$X_f = 3.175 - 8.25$ mm

In the case of correlations (6) and (10) the errors do not exceed ±15% for 91.3% of measuring points. For plain fins the correlation by Gray and Webb [20] was applied

$$j_H = 0.14\cdot Re_{Dc}^{-0.328}\cdot\left(\frac{P_t}{P_l}\right)^{-0.502}\cdot\left(\frac{s}{D_c}\right)^{0.0312} \tag{14}$$

The correlation (14) is applicable for

$N = 1 - 8$ or more

$Re_{Dc} = 500 - 24,700$

$P_t/D_c = 1.97 - 2.55$

$P_l/D_c = 1.70 - 2.58$

$s/D_c = 0.08 - 0.64$

The errors of correlation (14) do not exceed ±10% for 89% of measuring points. The Colburn number for heat transfer in Eqs. (6), (10) and (14) is expressed as

$$j_H = \frac{Nu_{exh}}{Re_{Dc}\cdot Pr_{exh}^{1/3}} \tag{15}$$

For selected circulating water mass flow rates and selected circulating water inlet temperatures the convection heat transfer coefficients for water were calculated using the following Gnielinski correlation [21]

$$Nu_w = \frac{(Re_{Di}-1000)\cdot Pr_w\cdot(f_w/2)}{1+12.7\cdot\sqrt{(f_w/2)}\cdot(Pr_w^{2/3}-1)} \tag{16}$$

where

$$Nu_w = \frac{h_w\cdot D_i}{k_w} \tag{17}$$

and

$$f_w = (1.58\cdot\ln(Re_{Di})-3.28)^{-2} \tag{18}$$

The correlations (16) and (18) are applicable for [21]

$Pr_w = 0.5 - 2000$

$Re_{Di} = 3000 - 5,000,000$

The errors of correlation (16) do not exceed ±10%. The errors of correlation (32) due to the errors of correlations (6), (10), (14) and (16) do not exceed ±5%. For the flow inside the tubes, the

characteristic dimension is the tube inside diameter D_i. The overall heat transfer coefficient is calculated from the equation below

$$UA = \left(\frac{1}{h_w \cdot A_i} + \frac{\delta_{wall}}{k_{wall} \cdot A_{wall}} + \frac{1}{\eta_s \cdot h_{exh} \cdot A}\right)^{-1} \quad (19)$$

where

$$A_{wall} = (A_e - A_i)/\ln(A_e/A_i) \quad (20)$$

The extended surface efficiency, η_s, was determined according to the standard procedure shown below.

$$\eta_s = 1 - \frac{A_f}{A} \cdot \left(1 - \eta_f\right) \quad (21)$$

where

$$\eta_f = \frac{\tanh(m \cdot r \cdot \phi)}{m \cdot r \cdot \phi} \quad (22)$$

$$m = \sqrt{\frac{2 \cdot h_{exh}}{k_f \cdot \delta_f}} \quad (23)$$

$$\phi = \left(\frac{R_{eq}}{r} - 1\right) \cdot \left[1 + 0.35 \cdot \ln\left(\frac{R_{eq}}{r}\right)\right] \quad (24)$$

$$R_{eq} = 1.27 \cdot \frac{P_t}{2} \cdot \left(\frac{\sqrt{(P_t/2)^2 + P_l^2}}{P_t} - 0.3\right)^{1/2} \quad (25)$$

Using the ε-NTU method, the heat exchanger performance was computed for selected combinations of input data. In the cases where the number of rows of tubes was greater than 6, the ε-NTU relationship for pure counterflow heat exchanger was applied [20]

$$\varepsilon = \frac{1 - \exp[-\mathrm{NTU} \cdot (1 - C^*)]}{1 - C^* \cdot \exp[-\mathrm{NTU} \cdot (1 - C^*)]} \quad (26)$$

Otherwise, for $N \leq 6$, the following expression was used [20]

$$\varepsilon = 1 - \exp\left\{\frac{\mathrm{NTU}^{0.22}}{C^*} \cdot \left[\exp\left(\frac{-C^*}{\mathrm{NTU}^{-0.78}}\right) - 1\right]\right\} \quad (27)$$

The heat capacity ratio in Eqs. (26) and (27), C^*, is defined as:

$$C^* = C_{min}/C_{max} \quad (28)$$

and is in the range from 0 to 1. The NTU is calculated as

$$\mathrm{NTU} = UA/C_{min} \quad (29)$$

The effectiveness of heat exchanger, ε, is defined as

$$\varepsilon = \dot{Q}/\dot{Q}_{max} \quad (30)$$

The maximum possible heat rate thermodynamically possible, $\dot{Q}_{max}$, is calculated from

$$\dot{Q}_{max} = C_{min} \cdot (T_{exh1} - T_{w1}) \quad (31)$$

The effectiveness of the HRU given by Eqs. (26) and (27) is the greater the smaller is C^*. For a given value of C^* the effectiveness increases asymptotically with the increase of NTU to a constant value. The HRU effectiveness determined from Eq. (26) or (27) is used to calculate the actual heat transfer rate $\dot{Q}$ from Eq. (30).

The data used in the calculations were included in the ranges

$$P_{el} = 2 - 30\ kW$$

$$T_{w1} = 308.15 - 343.15\ K$$

$$\dot{m}_w = 750 - 11{,}000\ kg/h$$

Thermophysical properties of fluids were determined for the mean temperature of the inlet and outlet of the exchanger. The temperature-dependent thermal conductivity of stainless steel AISI316, the heat exchanger material, was calculated from linear interpolation between the two values: 15.0 W/(m K) for 20 °C and 17.5 W/(m K) for 200 °C [22]. The thermal conductivity of copper was taken constant of 380 W/(m K). Thermophysical properties of water and exhaust gas were based on the data from Ref. [23]. The calculations assumed that the exhaust gas had properties of dry air with molar composition 78.12% N_2, 20.96% O_2 and 0.92% Ar. Due to the large excess air ratio (about 7.8 for REC and about 4.2 for NO REC at rated power, and even more at part-load) the effect of presence of combustion products on the thermophysical properties of the working medium is negligibly small, namely maximum of 2.00% difference in specific heats for REC and of 2.93% for NO REC case at ISO ambient conditions and at nominal power for which excess air ratio is minimal and the influence of combustion products is the greatest.

Influence of ambient temperature variation on the HRU performance may be included by introducing a correction factor, in case of availability of relevant data. Ambient temperature effect on the performance of HRU no. 8 (Table 1) has been tested for the rated power on the basis of data from Ref. [17]. The rise in ambient temperature of 5 K results in the 3% increase in the HRU performance, while the drop in ambient temperature of 5 K causes a decrease of the HRU performance by 5%. Overall, an increase in ambient temperature contributes to the HRU performance increase.

The backpressure effect resulting from the exhaust gas flow through the HRU is omitted as having no significant effect. Maximum pressure drop in the HRU is of magnitude of 300 Pa at the nominal power of microturbine. Such a pressure drop results in 0.4% decrease of power and 0.3% decrease of electrical efficiency [17]. Measurements of impact of backpressure on microturbine exhaust temperature [7] revealed that it is unnoticeable.

During normal operation of a microturbine it is not possible to recover the latent heat of the water vapor contained in the flue gas. Even when a natural gas is combusted in air taken from the ambient of temperature 35 °C fully saturated with moisture, the dew point temperature of the exhaust gas equals 41.5 °C for REC and 45.6 °C for NO REC. The present analysis was carried out for ISO ambient conditions and natural gas as a fuel. For such a case the dew point temperature of the exhaust gas drops to 27.1 °C and 35.3 °C for REC and NO REC, respectively. The lowest considered temperature of water at the exchanger inlet was 35 °C. The exhaust gas could not reach this temperature, so the condensation heat was not taken into account in the calculations. The excess air ratio is the larger the smaller the power developed by the microturbine, therefore at part load the dew point temperature is even lower. During the calculations, the following constraints for water were applied

$$Re_{Di} > 3000$$

$$T_{w2} < 368.15\ K$$

2.2. Regression analysis

The structure of the formula which approximates the dependence of the heat transfer rate of the HRU on the microturbine electrical output, the circulating water mass flow rate, and the circulating water inlet temperature was established by heuristic trial and error procedure. The effect of each independent variable on the HRU performance was examined. Many different mathematical formulas were tested while searching for a single universal function which is flexible, has as few coefficients as possible and gives results of acceptable accuracy. We started from a linear function with four coefficients, but the results were unsatisfactory. We gradually increased the number of correlation coefficients and correlation non-linearity until the accuracy criteria we had established were met.

The following approximating function was selected

$$\dot{Q} = e + a\cdot(P_{el}+b)^{g}\cdot T_{w1}^{d} - f\cdot P_{el}\cdot \dot{m}_{w}^{-c} \quad \left[\text{kW}\right] \tag{32}$$

In correlation (32) P_{el} should be expressed in [kW], T_{w1} in [K], and $\dot{m}_w$ in [kg/h]. To determine coefficients in Eq. (32) the following objective function was minimized

$$S = \sum_i w_i \cdot \frac{\left|\dot{Q} - \dot{Q}_i\right|}{\dot{Q}_i} \tag{33}$$

where $\dot{Q}_i$ is the heat transfer rate determined by the ε-NTU method for the i-th data set, $\dot{Q}$ is the heat transfer rate calculated from the approximate formula for the same data, and w_i is a weighting factor. The weighting factors, w_i, were used to reduce the maximum deviation of approximate values from the corresponding theoretical ones. For each considered case of a specific microturbine-HRU set, about 3000 points were used to determine the values of coefficients of the approximate expression. Calculations were performed using MathCAD 15.0 software. The values of coefficients in Eq. (32) for all investigated microturbine-HRU sets are given in Table 3. Relative approximation errors do not exceed 1.59% for 80% of the points. Larger errors occur for the smallest and largest values of P_{el}, T_{w1} and $\dot{m}_w$. The maximum relative error of any data point is 3.22%. The total error including the errors of correlations for heat transfer coefficients and approximation errors in Eq. (32) does not exceed 8.08% for all data points and 6.44% for 80% of the points. The RMS error for regression is calculated as

$$\text{RMS} = \sqrt{\frac{\sum_{i=1}^{n}\left(\dot{Q} - \dot{Q}_i\right)^2}{n}} \tag{34}$$

RMS was determined separately for each case. The maximum value of RMS occurred in case 10 and was equal to 1.34 kW.

When instead of the water mass flow rate, $\dot{m}_w$, the water outlet temperature, T_{w2}, is an input together with P_{el}, T_{w1}, the procedure of determining the thermal performance of the HRU, $\dot{Q}$, is as follows. From the equation

$$\dot{m}_w + C_1\cdot\dot{m}_w^{-c} - C_2 = 0 \tag{35}$$

$\dot{m}_w$ is determined, and then from the equation

$$\dot{Q} = \dot{m}_w\cdot q/3600 \tag{36}$$

$\dot{Q}$ is calculated, where

$$q = c_w\cdot(T_{w2} - T_{w1}) \tag{37}$$

Coefficients C_1 and C_2 are calculated, respectively, from the following relationships

$$C_1 = \frac{3600\cdot f\cdot P_{el}}{q} \tag{38}$$

$$C_2 = \frac{3600\cdot\left[e + a\cdot(P_{el}+b)^{g}\cdot T_{w1}^{d}\right]}{q} \tag{39}$$

In Eqs. (35)–(39) $\dot{Q}$ and P_{el} are expressed in [kW], q in [kJ/kg], $\dot{m}_w$ [kg/h], c_w [kJ/(kg·K)], temperatures in [K] and coefficients a–g [−].

3. Sample calculations

Sample calculations were performed to illustrate accuracy of the approximate expression and to demonstrate its usefulness for conducting various analyses of part-load performance of the microturbine-HRU sets.

Figs. 2–4 show the dependence of the heat transfer rate of the HRU to the circulating water, $\dot{Q}$, on the microturbine electrical power output, P_{el}, for particular cases of microturbine-HRU sets and selected inlet temperatures, T_{w1}, and flow rates, $\dot{m}_w$, of the circulating water. The lines represent values calculated from the approximate expression given by Eq. (32), the points represent exact values determined by the ε-NTU method. Agreement of the results is very good.

As seen in the figures, the amount of heat recovered in the heat exchanger, $\dot{Q}$, decreases with decreasing load, i.e., the decrease of electrical power from 30 kW to 2 kW results in the heat transfer rate reduction by a factor of 2.4–2.8 in the case of NO REC and of 3.5–4.2 in the case of REC. Reduction of $\dot{Q}$ is the greater the larger the surface of heat exchanger and the higher coefficients of heat transfer. For the REC cases, the heat transferred in the HRU depends almost linearly on load. In the NO REC case the heat transferred in the HRU is from 2.3 (high load) to 3.4 (low load) larger than in the REC case. The NO REC case yields higher thermal power because the

Table 3
Values of coefficients in approximate expression (32).

Case number	a	b	c	d	e	f	g
1.	768.51	18.002	0.75354	−1.0960	−9.3616	43.059	0.9145
2.	124.38	31.077	0.59773	−0.74638	−34.342	15.518	0.97036
3.	95.283	34.121	0.63420	−0.78873	−36.905	14.621	1.1083
4.	371.80	4.3178	0.51509	−0.20386	−116.47	27.260	0.17706
5.	481.28	4.9538	0.53063	−0.20317	−164.90	23.747	0.19536
6.	485.75	5.5688	0.60529	−0.23506	−148.25	22.726	0.23994
7.	91.713	30.190	0.51851	−0.79452	−32.577	15.879	1.1418
8.	99.184	29.774	0.59044	−0.82654	−31.223	14.960	1.1690
9.	435.99	6.6076	0.51556	−0.22095	−159.99	24.619	0.26353
10.	474.69	6.6058	0.60758	−0.20397	−187.68	22.743	0.23673

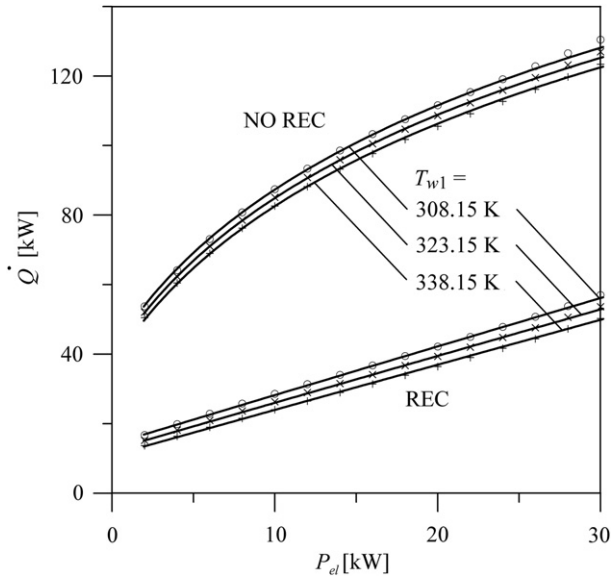

Fig. 2. Heat transfer rate of eight-row plain-fin HRU (cases no. 2 and 5) versus electrical power for various inlet water temperature at water mass flow rate of 5000 kg/h (points – calculated data; lines – approximation result).

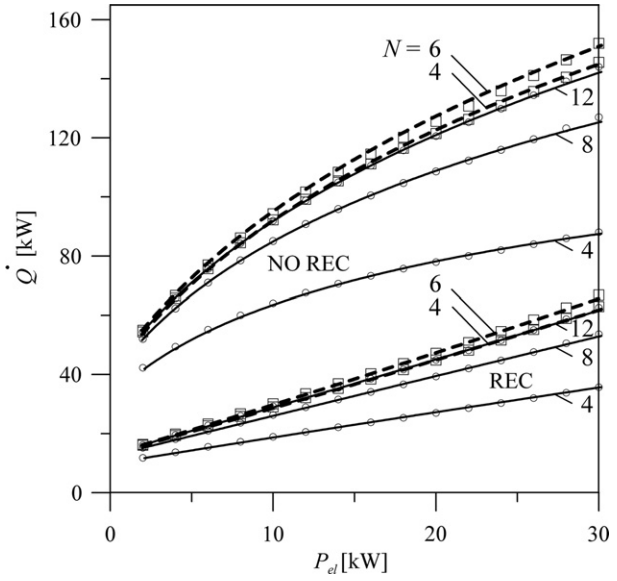

Fig. 4. Heat transfer rate of various HRUs versus electrical power at water mass flow of 5000 kg/h and inlet water temperature of 323.15 K (circles, squares – calculated data, lines – approximation result; solid lines and circles – plain fins, dashed lines and squares – wavy fins).

exhaust gases are not cooled in the internal recuperator and thus their temperature at the HRU inlet is higher. Moreover, in this case the exhaust gas mass flow rate is higher. The differences between the HRU performance profiles for REC and NO REC cases are due to differences in part-load characteristics of the REC and NO REC turbines as well as they result from different parameters of the exhaust gas for two cases under consideration.

The differences between the heat transfer rates for various water flow rates, numbers of tube rows in the exchanger, types of fins decrease with decreasing load. This follows from the fact that at low electrical loads, where the exhaust gas rates and its temperatures are low, the effectiveness of HRU, ε, is relatively high. In such cases the heat transfer rate is approximately equal to $\dot{Q}_{max}$ given by Eq. (31).

Lowering the temperature of water entering the heat exchanger (Fig. 2) as well as increasing the water rate (Fig. 3) or heat transfer surface (Fig. 4) results in increasing the heat transfer rate. For example, an increase of heat transfer surface of the heat exchanger with plain fins by 50%, from 8 to 12 tube rows, is followed by 14% increase of $\dot{Q}$ in the REC case at full electrical load.

As seen in Fig. 4, the copper wavy-fin HRU is more efficient than the stainless steel plain-fin HRU. It is mainly due to strongly reduced fin effectiveness resulting from low thermal conductivity of stainless steel.

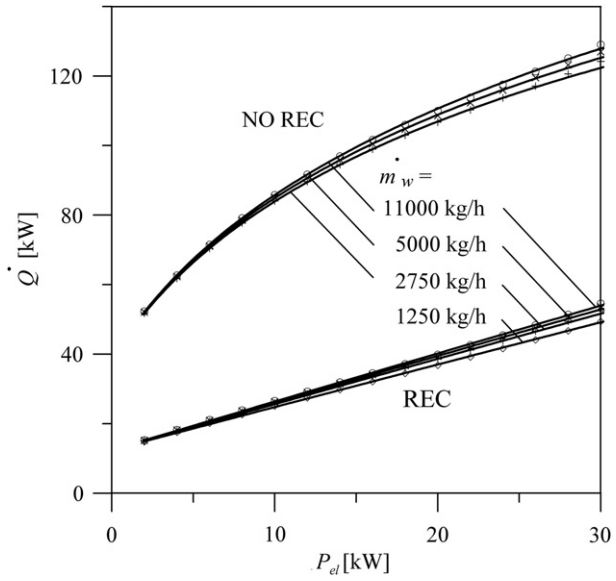

Fig. 3. Heat transfer rate of eight-row plain fin HRU (cases no. 2 and 5) versus electrical power for various water mass flow rate at inlet water temperature of 323.15 K (points – calculated data; lines – approximation result).

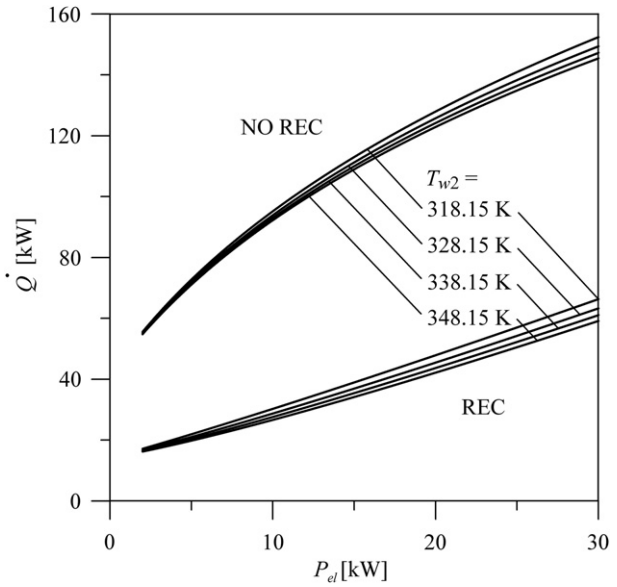

Fig. 5. Heat transfer rate of four-row wavy-fin HRU (cases no. 7 and 9) versus electrical power for various outlet water temperatures at inlet water temperature of 313.15 K.

Fig. 5 displays the dependence of $\dot{Q}$ on P_{el} for the case where the water outlet temperature, T_{w2}, is used as an input parameter instead of the water mass flow rate, $\dot{m}_w$. An increase in water outlet temperature results in a decrease of heat transfer rate because in this case the mean temperature difference and the water side heat transfer coefficient decrease. Data for Fig. 5 were calculated using the algorithm presented by formulas (35)–(39).

4. Conclusions

The performed analysis has shown that it is possible to formulate a versatile approximate expression, $\dot{Q} = \dot{Q}(P_{el}, \dot{m}_w, T_{w1})$, for calculation of heat transfer rate of the heat recovery unit, which is valid for various microturbine-HRU sets. Extension of the applicability of the proposed function for other sets than investigated in the work requires determining appropriate coefficients, which is a laborious task. Moreover, for other microturbine-HRU sets the function structure may not be optimal with respect to accuracy. In such cases the function structure should be adjusted to better fit the calculated data. Once the coefficients of correlation are calculated, the prediction of the amount of available heat at different loads can be done quickly and easily.

Fig. 2 shows that at low loads the HRU performance does not depend much on the circulating water mass flow rate. It therefore can be concluded that it is reasonable to reduce the circulating water flow along with decreasing load. In this way the pumping work is decreased with only slight reduction of transferred heat. The results of analysis show that the exchanger designed for a nominal load is also suitable for partial load.

Acknowledgements

This study was partly supported by the following project: The strategic program of scientific research and experimental development of the National (Polish) Centre for Research and Development: “Advances Technologies for Energy Generation”; Task 4. “Elaboration of Integrated Technologies for the Production of Fuels and Energy from Biomass as well as from Agricultural and other Waste Materials”.

References

[1] Colombo LP, Armanasco F, Perego O. Experimentation on a cogenerative system based on a microturbine. Appl Therm Eng 2007;27:705–11.
[2] Ge YT, Tassou SA, Chaer I, Suguartha N. Performance evaluation of a trigeneration system with simulation and experiment. Appl Energy 2009;86:2317–26.
[3] Ho JC, Chua KJ, Chou SK. Performance study of a microturbine system for cogeneration application. Renew Energy 2004;29:1121–33.
[4] Kaikko J, Backman J, Koskelainen L, Larjola J. Technical and economic performance comparison between recuperated and non-recuperated variable-speed microturbines in combined heat and power generation. Appl Therm Eng 2007;27:2173–80.
[5] Kaikko J, Backman J. Technical and economic performance analysis for a microturbine in combined heat and power generation. Energy 2007;32:378–87.
[6] Lee JJ, Jeon MS, Kim TS. The influence of water and steam injection on the performance of a recuperated cycle microturbine for combined heat and power application. Appl Energy 2010;87:1307–16.
[7] Pierce FE. Summary of results from testing a 30-kW-microturbine and combined heat and power (CHP) system. Oak Ridge (TN): Oak Ridge National Laboratory Integrated Energy System (IES) Test Laboratory; 2007 May. Report No.: DOE/EE-0316.
[8] Sanaye S, Ardali MR. Estimating the power and number of microturbines in small-scale combined heat and power systems. Appl Energy 2009;86:895–903.
[9] Zhang N, Cai R. Analytical solutions and typical characteristics of part-load performances of single shaft gas turbine and its cogeneration. Energy Convers Manage 2002;43:1323–37.
[10] Caresana F, Brandoni C, Feliciotti P, Bartolini CM. Energy and economic analysis of an ICE-based variable speed-operated micro-cogenerator. Appl Energy 2011;88:659–71.
[11] He X, Cai R. Typical off-design analytical performances of internal combustion engine cogeneration. Front Energy Power Eng China 2009;3:184–92.
[12] Kong XQ, Wang RZ, Wu JY, Huang XH, Huangfu Y, Wu DW, et al. Experimental investigation of a micro-combined cooling, heating and power system driven by a gas engine. Int J Refrigeration 2005;28:977–87.
[13] Lee DH, Lee JS, Park JS. Effects of secondary combustion on efficiencies and emission reduction in the diesel engine exhaust heat recovery system. Appl Energy 2010;87:1716–21.
[14] Possidente R, Roselli C, Sasso M, Sibilio S. Experimental analysis of micro-cogeneration units based on reciprocating internal combustion engine. Energy Build 2006;38:1417–22.
[15] Zhao XL, Fu L, Zhang SG, Jiang Y, Li H. Performance improvement of a 70 kWe natural gas combined heat and power (CHP) system. Energy 2010;35:1848–53.
[16] Badami M, Casetti A, Campanile P, Anzioso F. Performance of an innovative 120 kWe natural gas cogeneration system. Energy 2007;32:823–33.
[17] Capstone Turbine Corporation. Technical reference Capstone model C30 performance (410004 Rev. D), http://docs.capstoneturbine.com; 2006.
[18] Capstone Turbine Corporation. Capstone microturbine model 330 installation and start-up, http://www.globalmicroturbine.com; 2001.
[19] Wang CC, Hwang YM, Lin YT. Empirical correlations for hest transfer and flow friction characteristics of herringbone wavy fin-and-tube hest exchangers. Int J Refrigeration 2002;25:673–80.
[20] Kuppan T. Heat exchanger design handbook. New York: Marcel Dekker Inc; 2000. p. 42, 62, 197.
[21] Thome JR. Engineering data book III. Wolverine Tube Inc; 2010. p. 5–3.
[22] Lucefin Group. AISI316 stainless steel datasheet. http://www.trafilix.com/en_pdf/AISI316.pdf.
[23] Lemmon EW, McLinden MO, Huber ML. NIST reference fluids thermodynamic and transport properties – REFPROP 7.0, standard reference database 23. Gaithersburg: National Institute of Standards and Technology; 2002.